Journal of The Electrochemical Society, **147** (1) 368-372 (2000)
S0013-4651(99)10-006-5 CCC: $7.00 © The Electrochemical Society, Inc.

Reliability of Multistacked Chemical Vapor Deposited Ti/TiN Structure as the Diffusion Barrier in Ultralarge Scale Integrated Metallization

Po-Tsun Liu,[a,*] Ting-Chang Chang,[b,c,,z] J. C. Hu,[d] Y. L. Yang,[b] and S. M. Sze[a,b]**

[a]*Department of Electronics Engineering and Institute of Electronics, National Chiao-Tung University, HsinChu 300, Taiwan*
[b]*National Nano Device Laboratory, HsinChu 300, Taiwan*
[c]*Department of Physics, National Sun Yat-Sen University, Taiwan*
[d]*Department of Materials Science and Engineering, National Tsing-Hua University, HsinChu, Taiwan*

The reliability of multistacked titanium/titanium nitride (Ti/TiN) films as a diffusion barrier has been investigated by electrical characteristic measurements and material analyses. Both the chlorine content and the resistivity of the multistacked Ti/TiN films are significantly decreased when compared with a single layer of chemical vapor deposited-TiN film with the same thickness. The endurance of the diffusion barrier to thermal stress is enhanced by increasing the number of stacked layers of Ti/TiN films. Secondary ion mass spectroscopy depth profiles of the multistacked Ti/TiN samples showed that Ti atom distribution is fairly uniform in filling the grain boundary of the TiN film. The result is consistent with the observation of X-ray transmission microscopy. Therefore, the leakage current resulting from junction spiking is further reduced by the grain boundary effects when employing multistacked Ti/TiN as the diffusion barrier layer instead of a single layer of TiN film.
© 2000 The Electrochemical Society. S0013-4651(99)10-006-5. All rights reserved.

Manuscript received May 12, 1999.

Titanium nitride (TiN) has been widely used as a diffusion barrier and glue layer at the via/contact level to the diffusion barrier and also as an antireflection coating in aluminum metallization for several decades because of its high thermal stability, low electrical resistivity, good resistance to corrosion, and good diffusion barrier characteristics.[1-3] These properties allow TiN to withstand the repeated thermal cycles used in multilevel metallization of integrated circuit (IC) devices and make its continued use in deep submicrometer device technologies highly desirable. TiN film is traditionally deposited by physical deposition methods such as reactive ion sputtering or nitridation of sputter deposited it in nitrogen-containing gases at high temperatures.[4,5] However, the sputtering technique is inherently nonconformal, resulting in significant thinning at via and trench edges and walls. It therefore gives poor step coverage and could not meet the demands of ultralarge scale integrated (ULSI) technologies below the subquarter micron level. Chemical vapor deposition (CVD), on the other hand, offers conformal metal growth and the ability to coat large area substrates with excellent uniformity at industrially viable growth rates and potentially meet performance demands well into the 0.18 μm device technology and beyond.[6,7]

The commonly used precursors for CVD TiN processes are titanium tetrachloride ($TiCl_4$) associated with ammonia[8,9] and metallorganic titanium compounds such as tetrakis(dimethylamino)titanium (TDMAT)[10] and tetrakis(diethylamino)titanium (TDEAT).[11] Both TDMAT and TDEAT have been successfully used to deposit TiN films with good step coverage at temperatures below 400°C. However, the as-deposited films are porous and absorb moisture and oxygen when they are exposed to air, resulting in the degradation of film's electrical properties. These films also contain organic carbon and hydrogen,[12] and have much higher resistivity than those deposited by sputtering. Another disadvantage of the metallorganic precursors is that they could not be used to deposit metallic titanium films.

Low-temperature plasma assisted deposition of TiN film using the reaction between the inorganic precursor $TiCl_4$ and NH_3 has been be applied as a diffusion barrier for Al interconnects and an adhesion layer for W-plugs in the past decade. $TiCl_4$ is a colorless liquid and has a vapor pressure of about 12 Torr at room temperature. It has the lowest melting point (-23°C) and the highest vapor pressure among titanium halides. The high vapor pressure of $TiCl_4$ allows it to be delivered to the reaction chamber through a conventional mass flow controller, while the low-vapor pressure metallorganic CVD precursors require an expensive liquid delivery and flash vaporization system. In addition, $TiCl_4$ is used as a precursor for titanium deposition. In the $TiCl_4/NH_3$ based CVD-TiN process, however, the incorporation of a significant amount of chlorine (Cl) in the film is of major concern for long-term reliability of finished devices.[13,14] On the other hand, the TiN grains were columnar structures.[15-17] When TiN was used as a barrier layer, Al and Si would interdiffuse through the grain boundaries of the TiN film after being subjected to thermal stress at elevated temperatures. The interdiffusion of Al and Si through the barrier caused junction spiking, which exhibited a large leakage current or even electrical shorting. Therefore, it is necessary to improve the film properties of CVD-TiN.

In this work, a reliable CVD multistacked Ti/TiN structure with *in situ* NH_3 plasma post-treatment is proposed to enhance the barrier property of TiN films and reduce both the resistivity and chlorine content of TiN films simultaneously. Material analyses and leakage current measurements were used to investigate the characteristics of the multistacked Ti/TiN structure.

Experimental

The Al/TiN/$TiSi_2$/n^+-p and Al/(stacked Ti/TiN)/$TiSi_2$/n^+-p junction diodes were fabricated for the investigation of a single CVD-TiN and a multistacked Ti/TiN barrier capability. The starting materials were 6 in., (100)-oriented p-type silicon wafers. After RCA standard cleaning, the wafers were thermally oxidized at 1050°C in a steam atmosphere to grow a 550 nm oxide layer. The contact holes were patterned by photolithographic and reactive ion etching (RIE) techniques. For the n^+-p junction, the p-type substrate implantation was carried out by BF^{2+} implant at 50 keV to a dose of 2.5×10^{15} cm^{-2} while the junction implantation was carried out by As^+ implant on p-type substrate at 40 keV to a dose of 5×10^{15} cm^{-2}. These samples were followed by furnace annealing at 800°C for 20 min in N_2 ambient and rapid thermal annealing (RTA) at 1050°C for 20 s.

After the junctions were formed, the wafers were prepared for Ti and TiN or multistacked Ti/TiN barrier layer deposition. In this study, both CVD-Ti and CVD-TiN films were deposited using a cluster tool which has two vacuum cassette elevators, a soft sputter etch module, a CVD Ti and a CVD TiN module, and a cool down station. The titanium films were deposited by plasma-enhanced chemical vapor deposition (PECVD) at a temperature of 590°C using a mixture of $TiCl_4$, H_2, and Ar. The process chamber pressure was 5 Torr and the rf power was 350 W. Metallic Ti and $TiSi_2$ films were formed in contact holes. Sequentially, samples were transferred to another chamber without exposure to atmosphere-depositing TiN

* Electrochemical Society Student Member.
** Electrochemical Society Active Member.
[z] E-mail: tcchang@ndl.gov.tw

Downloaded on 2014-04-28 to IP 140.113.38.11 address. Redistribution subject to ECS terms of use (see ecsdl.org/site/terms_use) unless CC License in place (see abstract).

S0013-4651(99)10-006-5 CCC: $7.00 © The Electrochemical Society, Inc.

films by LPCVD using $TiCl_4$ and NH_3 associated with a N_2 dilution gas. The base vacuum level of the CVD chamber was maintained to be better than 10^{-6} Torr. Total pressure was fixed at 20 Torr when LPCVD TiN film was deposited. The substrate temperature during TiN film growth was maintained at 630°C. The *in situ* NH_3 plasma post-treatment with 500 W was applied to as-deposited TiN films for 300 s. The $TiN/TiSi_2/n^+$-p junction diodes were thereby formed, which were also labeled as the standard sample (STD). On the other hand, the multistacked Ti/TiN films were formed by alternately depositing PECVD Ti and LPCVD TiN film on the $TiN/TiSi_2/n^+$-p substrate with a deposited period of 60 and 20 s, respectively. Consequentially, $TiN/Ti/TiN/TiSi_2/n^+$-p, $TiN/Ti/TiN/Ti/TiN/TiSi_2/n^+$-p, and $TiN/Ti/TiN/Ti/TiN/Ti/TiN/TiSi_2/n^+$-p samples associated with NH_3 plasma post-treatment for 300 s were manufactured and labeled as sample I, sample II, and sample III, respectively. The total thickness of these multistacked Ti/TiN films was 35 nm, the same as the sample STD, which was confirmed by X-ray transmission electron microscopy (XTEM). After the barrier layer deposition, aluminum alloy (Al-0.5 atom % Cu) was sputter deposited on the TiN and multistacked Ti/TiN barrier metal, respectively.

To investigate thermal stability of Al-Cu/$TiN/TiSi_2/n^+$-p and Al-Cu/(stacked Ti/TiN)/$TiSi_2/n^+$-p junction diodes, the diodes were subjected to thermal annealing at various temperatures ranging from 400 to 600°C for 30 min in N_2 ambient. Leakage currents of n^+-p diodes were measured by a staircase voltage ramp using an HP4145B semiconductor parameter analyzer at reverse bias voltage of 5 V for the barrier study of this contact system. At least 30 diodes were measured in each case. For material analysis, unpatterned samples of barrier/Si structures were also prepared. Sheet resistance of the multilayer structures was measured using a four-point probe, with 51 points measured. Chlorine concentration in barrier films was measured by Auger electron spectroscopy (AES) measurements. XRD analysis using a 30 keV copper Kα radiation was employed for phase identification.

Results and Discussion

In situ NH_3 plasma post-treatment is effective in reducing the resistivity of TiN films. Specific details were given in our earlier paper.[14] For the investigation of multistacked Ti/TiN films, the resistivity of all samples with a thickness of 35 nm was first measured. Figure 1 shows the resistivity of these samples as a function of the layer number of stacked Ti/TiN films. The resistivity of these samples with the same thickness was decreased with the increase in the layer number of stacked Ti/TiN films. This shows that the increasing layer number of stacked Ti/TiN films associated with NH_3 plasma post-treatment effectively contribute to reduce the resistivity of CVD-TiN films.

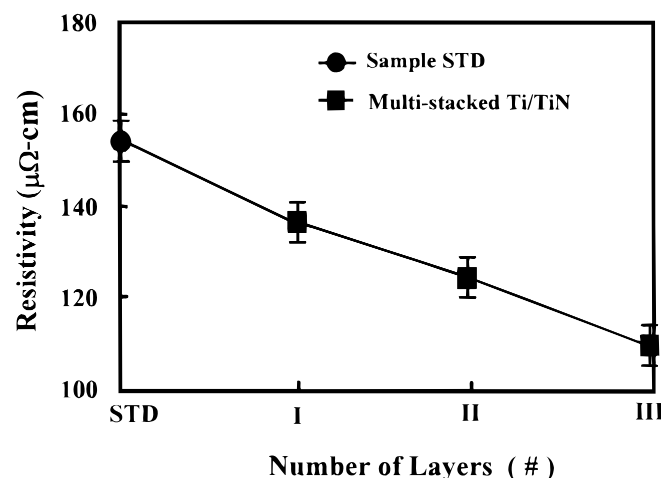

Figure 1. The resistivity of various samples with *in situ* NH_3 plasma post-treatment for 300 s. Samples are labeled as followed: CVD-$TiN/TiSi_2$/Si (sample STD), CVD-$TiN/Ti/TiN/TiSi_2$/Si (sample I), CVD-TiN/Ti/TiN/TiN/$Ti/TiSi_2$/Si (sample II), and CVD-$TiN/Ti/TiN/Ti/TiN/Ti/TiN/TiSi_2$/Si (sample III). The thickness of all samples is 35 nm.

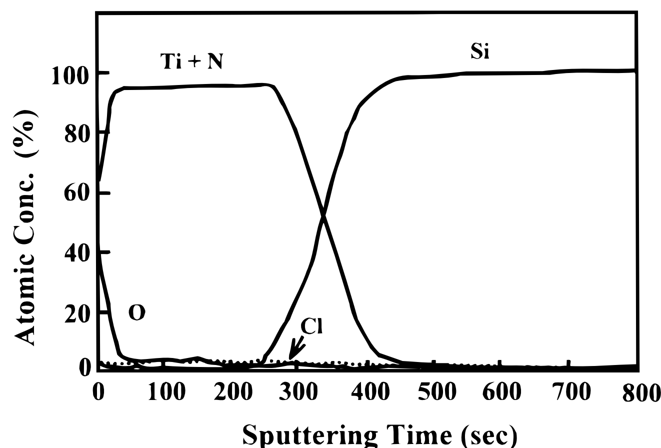

Figure 2. AES depth profile of a $TiN/TiSi_2$/Si sample with NH_3 plasma treatment for 300 s.

Furthermore, the chlorine content in these samples was detected by the analysis of AES depth profile. Figure 2 shows the AES depth profile of sample STD. The chlorine concentration in the sample STD was found to be about 2.9 atom %. As a result, the sample STD had a higher value of resistivity (~150 μΩ-cm). In contrast, the AES depth profile of sample III is revealed in Fig. 3. The chlorine concentration in the sample III was detected to be about 1.6 atom %, which was lower than that of sample STD. A previous study showed that chlorine content in excess of 5 atom % would degrade metal reliability and increase resistivity of TiN film.[9] The chlorine content in the multistacked Ti/TiN film was close to 1.6 atom %. This will eliminate the corrosion in subsequent Al film. In addition, it was observed that the concentration of Ti + N was fairly uniformly in sample III according to AES measurements.

To investigate Ti atom distribution behavior in multistacked Ti/TiN films, the ^{47}Ti + N and ^{51}Ti depth profiles were measured by secondary ion mass spectrometry (SIMS) for an as-deposited multistacked sample III, as shown in Fig. 4. It was found that the distribution of Ti atoms is fairly uniformly in multistacked Ti/TiN sample. The result is also in agreement with the observation of XTEM image. Figure 5a and b show the cross-sectional XTEM image of sample STD and sample III, respectively. The interfaces between TiN and $TiSi_2$ in sample STD are rather smooth. In addition, it is clearly observed that the CVD-TiN grains are columnar structures, which is consistent with previous documents.[13-15] The

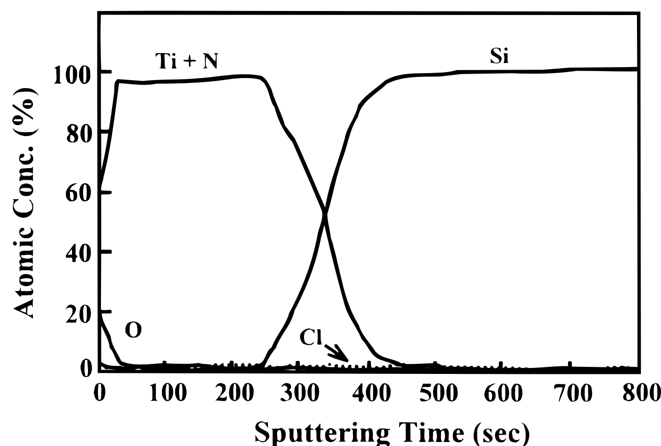

Figure 3. AES depth profile of $TiN/Ti/TiN/Ti/TiN/Ti/TiN/TiSi_2$/Si sample after being treated with NH_3 plasma for 300 s.

Downloaded on 2014-04-28 to IP 140.113.38.11 address. Redistribution subject to ECS terms of use (see ecsdl.org/site/terms_use) unless CC License in place (see abstract).

S0013-4651(99)10-006-5 CCC: $7.00 © The Electrochemical Society, Inc.

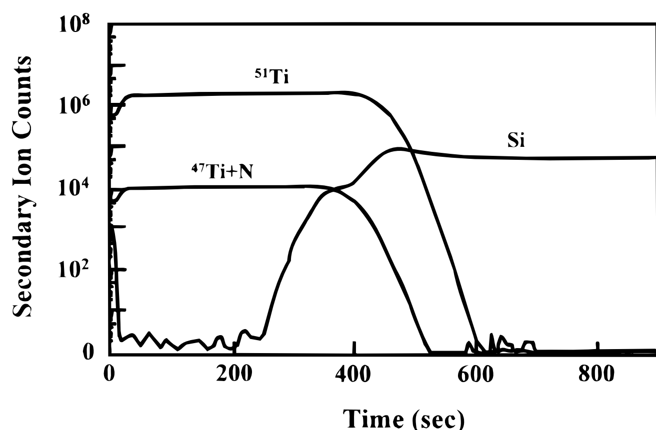

Figure 4. SIMS depth profiles of TiN/Ti/TiN/Ti/TiN/Ti/TiN/$TiSi_2$/Si sample after being treated with NH_3 plasma for 300 s.

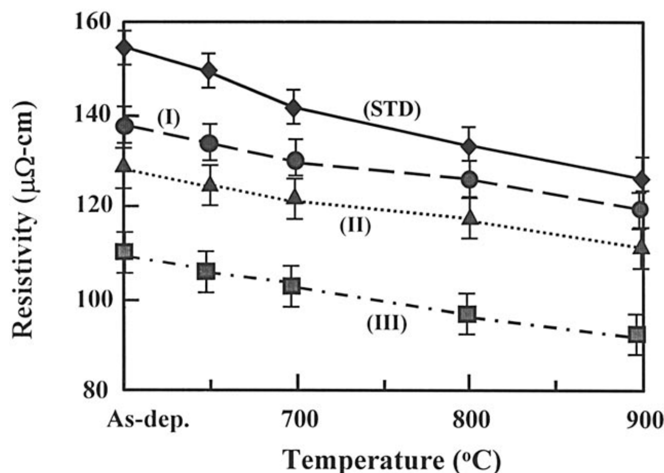

Figure 6. Resistivity of various multistacked Ti/TiN samples as a function of RTA temperature for 60 s.

average grain size of CVD-TiN film was also measured to be about 20 nm by a plan-view observation of micrograph image. For multistacked Ti/TiN films in sample III, the cross-sectional XTEM image also shows the rather smooth interfaces between TiN and $TiSi_2$. However, the TiN grain boundaries and interfaces between Ti and TiN film in multistacked Ti/TiN structure does not seem to be apparent in the XTEM image, which means that subsequent deposition of Ti may stuff into the CVD-TiN grain boundaries. This is also consistent with SIMS data that Ti atoms are distributed fairly uniformly by fast diffusion in TiN films of multistacked structure. In addition, a previous study has shown that the PECVD Ti deposition rate varied with different substrate.[18] Except for amorphous and crystal Si, the deposition rate of PECVD Ti is rather low on other substrates. As a result, the thickness of PECVD Ti deposited on TiN film for 20 s to form multistacked Ti/TiN films is relatively thin. On the basis of the above statements, it is reasonably believed that the very thin layer of PECVD Ti layer can effectively fill the grain boundary of TiN films to reduce film resistivity. Additionally, the resistively of multistacked Ti/TiN film can be decreased further by a rapid thermal annealing (RTA) treatment. Figure 6 shows the resistivity of these multi-stacked Ti/TiN samples after a RTA treatment at various temperatures for 60 s. It is found that the resistivity of sample III can be reduced to 75 μΩ-cm. However, the resistivity of sample STD was only reduced to about 130 μΩ-cm. A previous study[19] showed that the RTA-induced grain sintering leads to a tighter grain boundary structure and thus enhances the CVD-TiN barrier properties, which is of great importance for the deep submicronmeter technology with Al plug or Cu metallization. In our study, RTA treatment certainly improves the film quality of multistacked Ti/TiN film. Figure 7 shows the plan-view grain structure of multistacked sample III after RTA treatment at 900°C for 60 s. The average grain size was measured to be about 30 nm, which was larg-

(a)

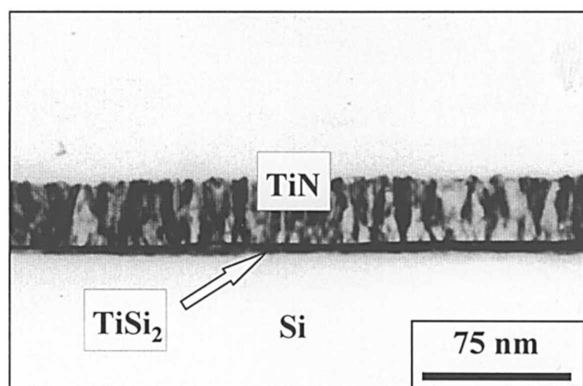

(b)

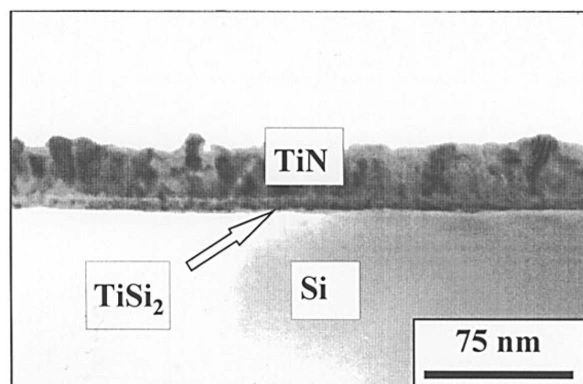

Figure 5. Cross-sectional XTEM micrographs for different samples of the same thickness (35 nm); (a) CVD-TiN/$TiSi_2$/Si (sample STD) and (b) CVD-TiN/Ti/TiN/Ti/TiN/Ti/TiN/$TiSi_2$/Si (sample III).

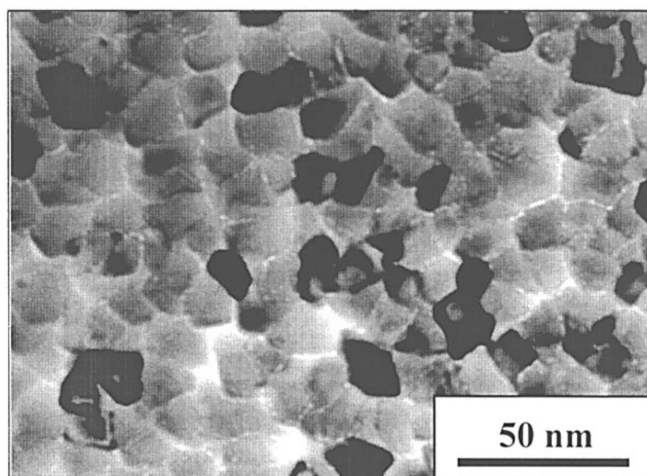

Figure 7. Plan-view image of multistacked TiN/Ti/TiN/Ti/TiN/Ti/TiN/$TiSi_2$/Si sample treated with *in situ* NH_3 plasma followed by RTA treatment at 900°C for 60 s.

Downloaded on 2014-04-28 to IP 140.113.38.11 address. Redistribution subject to ECS terms of use (see ecsdl.org/site/terms_use) unless CC License in place (see abstract).

S0013-4651(99)10-006-5 CCC: $7.00 © The Electrochemical Society, Inc.

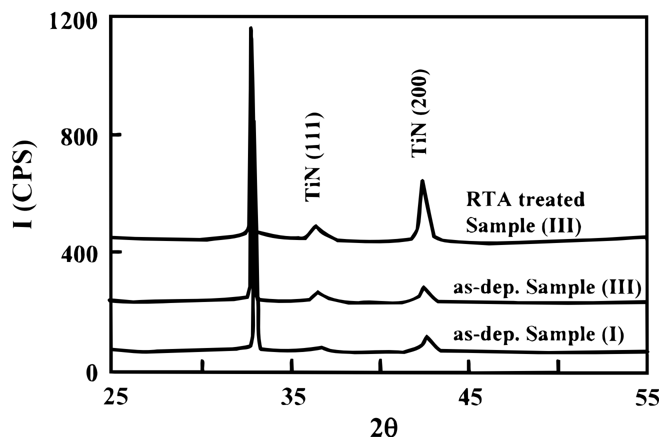

Figure 8. XRD spectra of RTA treated sample III, as-deposited sample III, and as-deposited sample STD. The wavelength of the Cu Kα X-ray is 0.15405 nm.

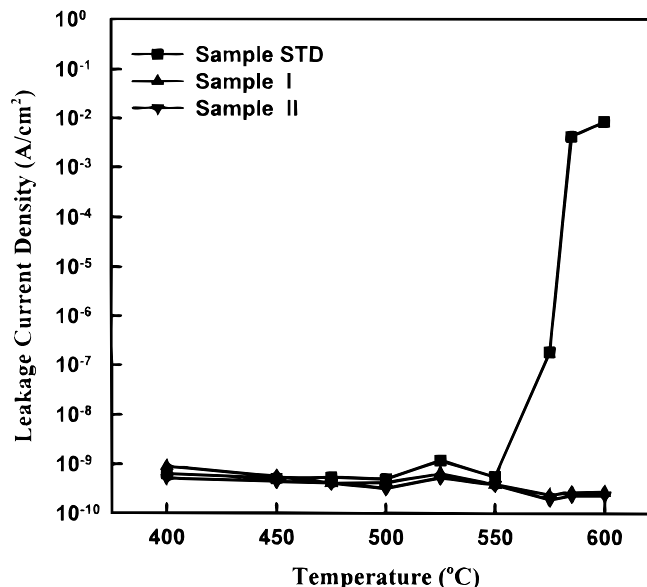

Figure 9. Leakage current density of n^+-p junction diodes with various types of barrier layer.

er than that of as-deposited multistacked Ti/TiN film (20 nm). As a result, low resistivity (<100 μΩ-cm) of CVD-TiN film can be achieved by the RTA treatment. In addition, XRD analysis was applied to investigate the crystal orientation of CVD-TiN films, as shown in Fig. 8. The textural variations observed might have significant implications for the barrier characteristics. XRD spectrum of multi-stacked Ti/TiN film reveals significant textures of (002) and (111) orientation. Compared with the XRD spectrum for sample STD, a stronger (111) orientated TiN was found in sample III. In addition, it was observed that the intensity of (002) and (111) orientation was increased with the RTA treatment due to TiN grain growth. Fiordalice *et al.*[20] reported that the texture of the TiN film can significantly affect that of the overlaying aluminum film. A (111)-orientated TiN film produces an identical aluminum orientation. This effect is important since predominantly (111)-orientated aluminum exhibits enhanced electromigration resistance. Accordingly, in our study stronger (111) peak implies that the barrier property of multistacked Ti/TiN film is superior to that of single layer of CVD-TiN film (sample STD).

Barrier capability of the multistacked Ti/TiN structure was investigated by evaluating the thermal stability of n^+-p junction diodes using electrical measurements. Figure 9 illustrates the leakage current density measured at a reverse bias voltage of 5 V for different multistacked Ti/TiN structures annealed at 400∼600°C for 30 min. The Al-Cu/Sample STD/n^+-p diodes remained stable after annealing at temperatures up to 550°C but suffered moderate degradation of electrical characteristics at 575°C; annealing at 600°C resulted in severe degradation. This indicates that thermal stability of the Al-Cu/sample STD/n^+-p junction diodes is severely degraded by the interdiffusion between Al atoms and Si through the columnar-grains of TiN films leading to junction spiking, which will exhibit a large leakage current or even electrical shorting. The barrier properties of CVD-TiN film can be significantly improved by multistacked Ti/TiN structure with the same thickness. For the diodes with a stacked Ti/TiN barrier, the devices remained stable after annealing at temperatures up to 600°C. Experimental results show that the thermal stability of multistacked Ti/TiN films is superior to a single layer of CVD-TiN film. These results are believed to show that the very thin PECVD Ti layer deposited on TiN film in multistacked Ti/TiN structure may fill the grain boundaries of columnar TiN film to reduce paths for Al/Si interdiffusion. This would make it difficult for junction spiking. As a result, the leakage current of n^+-p junction with multistacked Ti/TiN as barrier is lower than that of a single layer of CVD-TiN film. This explanation is also in agreement with the observation of uniformly distributed Ti in SIMS depth profile, as shown in Fig. 4. Therefore, the CVD multistacked Ti/TiN structure is really effective in enhancing the barrier properties.

Conclusion

In this work, a multistacked Ti/TiN structure has been proposed to enhance the barrier properties against the interdiffusion of aluminum and Si resulting in junction spiking. By increasing the number of layers of Ti/TiN films associated with NH_3 plasma post-treatment, both the resistivity and chlorine content (<2 atom %) in TiN films were effectively reduced. Extremely low chlorine concentration would minimize corrosion in subsequent aluminum film. In addition, low resistivity less than 100 μΩ-cm can be achieved by RTA treatment. SIMS depth profiles of the multistacked Ti/TiN sample show that the Ti atom distribution is fairly uniform in filling the grain boundary of TiN films, which is agreement with the observation of XTEM. This would effectively reduce the paths for Al/Si interdiffusion. XRD spectrum also showed stronger (111)-orientated TiN appear in the multistacked Ti/TiN structure than that of a single layer of CVD-TiN film. This (111) orientation would enhance the electromigration resistance of aluminum wires. In addition, electrical measurements indicated the barrier property of multistacked Ti/TiN film is superior to that of a single layer of CVD-TiN film. For the n^+-p junction diodes with a multistacked Ti/TiN barrier, the devices remained stable after annealing at temperatures up to 600°C while severe degradation occurred in that of a single layer of CVD-TiN barrier of the same thickness.

Acknowledgment

This work was performed at the National Nano Device Laboratory and the National Science Council of the Republic of China under contract, No. NSC88-2215-E-317-009.

National Chiao-Tung University assisted in meeting the publication costs of this article.

References

1. R. I. Hegde, R. W. Fiordalice, E. O. Travis, and R. J. Tobin, *J. Vac. Sci. Technol., B,* **11,** 1287 (1993).
2. J. S. Byun, C. R. Kim, K. G. Rha, and J. J. Kim, *Jpn. J. Appl. Phys.,* **34,** 978 (1995).
3. J. T. Hillman, R. Foster, J. Faguet, W. Triggs, R. Arora, and M. Ameen, *Solid State Technol.*, 147 (July 1995).
4. A. Intemann, H. Koerner, G. Ruhl, K. Hieber, and E. Hartmann, in *Advanced Metallization for ULSI Applications-X,* R. Blumenthal and G. Jenssen, Editors, p. 209, Materials Research Society, Pittsburgh, PA (1995).
5. J. M. Fu, M. Narasimhan, G. D. Yao, X. Xu, and F. Chen, in *Proceedings of the 12th International VLSI Multilevel Interconnection Conference,* p. 198 (1995).
6. C. Faltermeier, C. Goldberg, M. Jones, A. Upham, D. Manger, G. Peterson, J. Lau, and A. E. Kaloyeros, *J. Electrochem. Soc.,* **144,** 1002 (1997).
7. J. Hu, M. Ameen, G. Leusink, D. Webb, and J. T. Hillman, *Thin Solid Films,* **308-309,** 589 (1997).

Downloaded on 2014-04-28 to IP 140.113.38.11 address. Redistribution subject to ECS terms of use (see ecsdl.org/site/terms_use) unless CC License in place (see abstract).

S0013-4651(99)10-006-5 CCC: $7.00 © The Electrochemical Society, Inc.

8. J. Laimer, H. Stori, and P. Rodhammer, *J. Vac. Sci. Technol.,* **A-7,** 2952 (1989).
9. N. J. Ianno, A. U. Ahmed, and D. E. Englebert, *J. Electrochem. Soc.,* **136,** 276 (1989).
10. A. Paranjpe and M. L. Raja, *J. Vac. Sci. Technol., B,* **13,** 2105 (1995).
11. S. C. Sun and M. H. Tsai, *Thin Solid Films,* **253,** 440 (1994).
12. J. T. Hillman, M. J. Rice, Jr., D. W. Studiner, R. F. Foster, and R. W. Fiordalice, in *Proceedings of the 9th International VLSI Multilevel Interconnection Conference,* p. 246 (1992).
13. T. Suzuki, T. Ohba, Y. Furumura, and H. Tsutikawa, in *Proceedings of the 10th International VLSI Multilevel Interconnection Conference,* p. 418 (1993).
14. Y. J. Mei, T. C. Chang, J. C. Hu, L. J. Chen, Y. L. Yang, F. M. Pan, W. F. Wu, A. Ting, and C.Y. Chang, *Thin Solid Films,* **308,** 594 (1997).
15. D. Liao, Y. lin, H. Yang, H. Witham, J. May, J. lee, and S. Tso, in *Proceedings of the 11th International VLSI Multilevel Interconnection Conference,* p. 428 (1994).
16. G. Dixit, C. Wei, and F. Liou, *Appl. Phys., Lett.,* **62,** 357 (1993).
17. K. Ngan, R. Mosely, Z. Xu, and I. Raaijmakers, *Mater. Res. Soc. Symp. Proc.,* **337,** 249 (1994).
18. T. Taguwa, K. Urabe, K. Ohto, H. Gomi, in *Proceedings of the 14th International VLSI Multilevel Interconnection Conference,* p. 255 (1997).
19. X. W. Lin, S. Bothra, L. Topete, D. Pramanik, in *Proceedings of the 14th International VLSI Multilevel Interconnection Conference,* p. 443 (1997).
20. R. W. Fiordalice, R. I. Hegde, and H. Kawasaki, *J. Electrochem. Soc.,* **143,** 2059 (1996).

Downloaded on 2014-04-28 to IP 140.113.38.11 address. Redistribution subject to ECS terms of use (see ecsdl.org/site/terms_use) unless CC License in place (see abstract).